Simulated impact of intraseasonal variations in surface heat and momentum fluxes on the pelagic ecosystem of the Arabian Sea

Michio Kawamiya[1] and Andreas Oschlies
Institut für Meereskunde an der Universität Kiel, Kiel, Germany

Received 23 August 2003; revised 19 December 2003; accepted 20 January 2004; published 6 March 2004.

[1] A series of numerical experiments using a three-dimensional, coupled ecosystem-circulation model has been performed to evaluate the impact of variations on an "intraseasonal" daily to monthly timescale in surface fluxes of heat and momentum on simulated biological production in the Arabian Sea. The biological component is a four-compartment, nitrogen-based system; the physical component is a high-vertical-resolution *z*-level model that includes a mixed-layer model based on the turbulent energy equation and contrasts with layer models which often overestimate vertical mixing associated with intraseasonal mixed-layer retreat and formation. Experiments show that the intraseasonal variations in the forcing may have to be considered when comparing sparsely sampled data with results from a numerical model. The experiments provide, however, no evidence that there is any rectification impact on longer timescales. In particular, accounting for intraseasonal variations has essentially no effect on the simulated annual mean biological production. *INDEX TERMS:* 4815 Oceanography: Biological and Chemical: Ecosystems, structure and dynamics; 4842 Oceanography: Biological and Chemical: Modeling; 4845 Oceanography: Biological and Chemical: Nutrients and nutrient cycling; 4572 Oceanography: Physical: Upper ocean processes; 4568 Oceanography: Physical: Turbulence, diffusion, and mixing processes; *KEYWORDS:* intraseasonal variations, Arabian Sea, ecosystem

Citation: Kawamiya, M., and A. Oschlies (2004), Simulated impact of intraseasonal variations in surface heat and momentum fluxes on the pelagic ecosystem of the Arabian Sea, *J. Geophys. Res.*, *109*, C03016, doi:10.1029/2003JC002107.

1. Introduction

[2] Modeling nature requires a process of selection. When one conducts a computer simulation of a certain phenomenon, it is infeasible to incorporate all the possibly relevant events occurring in reality. In some cases, however, the selection is not straightforward. An example is the consideration of "intraseasonal" daily to monthly variations of surface forcing for a basin-scale, long-term simulation of the ocean. Most numerical ecosystem-circulation simulations so far have been carried out using slowly varying monthly climatological forcing. This might be a reflection of quite successful simulations without intraseasonal variations and the lack of reliable data and disk space, but it does not necessarily mean that shorter-term variations on daily to monthly timescales, such as sudden peaking in wind and convection due to a cold wave, are playing no role.

[3] Some recent modeling studies investigate the role of such short-term variations. *Large and Crawford* [1995] succeeded in reproducing a large and rapid cooling of the surface ocean generated by the passage of a storm using one-dimensional mixed-layer models. The cooling reaches $\sim$1.0°C in one day. Such a large response could have an impact on the surface ocean on a longer timescale. *Ridderinkhof* [1992] used data sets with various timescales to force a one-dimensional model for a coastal region with surface and bottom mixed-layer models of the bulk type and found that the incorporation of short-term variations affects long-term characteristics such as heat storage of a water column. He also speculated that events with short timescales may have an influence on biological production. More recently, *McCreary et al.* [2001] performed a comparative study by running a layered physical-biological model of the Arabian Sea with and without short-term variations in surface forcing. They demonstrated that the intraseasonal variation prolongs the duration of spring bloom, thereby improving the agreement between the model results and observations in comparison with the earlier work of *McCreary et al.* [1996]. *McCreary et al.* [2001] cautioned, however, that some of their results could be model dependent. Specifically, because of the layer formulation of their model, nutrients underneath the surface mixed layer may be replenished too rapidly at times when the mixed layer (ML) retreats. They emphasized the necessity to examine the mixing process below the ML, arguing that there do exist some indications that such an efficient nutrient transport as simulated by their layer model can occur in reality.

[4] In the present study, results from another model of the Arabian Sea are provided with the purpose of investigating the effect of intraseasonal variations in surface forcing. The specific configurations of the present model are very different from those of *McCreary et al.* [2001] and may serve

[1]Now at Frontier Research System for Global Change, Showamachi, Kanazawa-ku, Yokohama, Japan.

0148-0227/04/2003JC002107$09.00

as a test of the generality of the importance of intraseasonal variations that they pointed out. It will be shown that results from the current model are similar to those of *McCreary et al.* [2001], in that intraseaonal variations are essential for pursuing an accurate match between model results and data, with one of the differences being that according to our model results, they have negligible effect on phenomena on seasonal or longer timescales.

2. Model Description

2.1. Structure

[5] Here we describe the model structure only briefly. For further details the reader is referred to *Kawamiya* [2001], *Kawamiya and Oschlies* [2003], and particularly regarding the biological model, *Oschlies and Garçon* [1999].

[6] For the physical component of the model, we adopt the modular ocean model version 2.1 developed by the Geophysical Fluid Dynamics Laboratory [*Pacanowski*, 1995], which has been set up for the Indian Ocean by *Rix* [1998]. The model domain extends from 30°S to 26°N and from 30°E to 110°E with a realistic bottom topography. Its meridional and zonal resolutions are both 1/3°. There are 35 vertical levels, 10 of which are within the upper 110 m. Horizontal diffusion and viscosity are expressed through a biharmonic operator with a coefficient of 2.5×10^{19} cm^4/s for both.

[7] To parameterize vertical mixing, we use the turbulence closure scheme of *Gaspar et al.* [1990] as adapted by *Blanke and Delecluse* [1993] to an ocean general circulation model, with a few minor modifications described by *Oschlies and Garçon* [1999] and *Kawamiya and Oschlies* [2003]. It computes vertical diffusivities and viscosities both within and below the surface mixed layer from the prognostically solved turbulent kinetic energy (TKE) and vertical stratification. We note that the parameterization by *Pacanowski and Philander* [1981] was used for vertical mixing in our preceding paper [*Kawamiya and Oschlies*, 2003], where we found that the *Pacanowski and Philander* [1981] parameterization yielded too little primary production in the central Arabian Sea. Primary production in the experiments with the *Gaspar et al.* [1990] turbulent closure is significantly higher and closer to, for example, the observational estimate by *Marra et al.* [1998] at 15.5°N, 61.5°E (see Figure 3a). The turbulent closure scheme results in a higher primary production because it generates deeper mixed layers during the southwestern monsoon (SWM) and larger diffusivities below the mixed layer (0.3 cm^2/s as opposed to 0.1 cm^2/s by the *Pacanowski and Philander* [1981] parameterization) throughout the year. The sensitivity of the modeled primary production to the choice of a vertical mixing scheme is discussed in more detail by *Kawamiya and Oschlies* [2003].

[8] The biological model used is based on nitrogen and has four compartments, that is, nitrate, phytoplankton, zooplankton, and detritus. The model variables evolve with time according to a set of advection-diffusion equations with source-minus-sink terms representing the biological interactions. Parameter values are the same as in the work by *Kawamiya and Oschlies* [2003].

2.2. Forcing

[9] Four main experiments are carried out in this study, as listed in Table 1, with two additional sensitivity experiments that are referred to in the discussion section. They are driven by two sets of background (monthly mean) winds, each with and without intraseasonal anomalies.

Table 1. Main and Sensitivity Experiments Performed in This Study

Code	Surface Forcing
	Main Experiments
MC	monthly mean climatology
DC	daily mean based on climatology
MY	monthly mean for the years 1994–1995
DY	daily mean for the years 1994–1995
	Sensitivity Experiments
DY-S1	same as DY but with monthly mean for heat flux for 1994–1995
DY-S2	same as DY but with monthly mean for wind stressandfriction velocity for 1994–1995

[10] Experiment monthly climatology (MC) is forced with "climatological" data computed from actual forcing data and averaged over the admittedly short period 1986–1988. Its heat flux Q is computed following [*Haney*, 1971],

$$Q = Q_{\mathrm{obs}} - \left(\frac{\partial Q}{\partial T}\right)_{\mathrm{obs}} (\mathrm{SST}_{\mathrm{obs}} - \mathrm{SST}_{\mathrm{model}}), \qquad (1)$$

where Q_{obs} is the observed heat flux, $(\partial Q/\partial T)_{\mathrm{obs}}$ is the coupling coefficient, $\mathrm{SST}_{\mathrm{obs}}$ is the observed sea surface temperature (SST), and $\mathrm{SST}_{\mathrm{model}}$ is the model SST. Surface salinity is relaxed to the monthly mean values of *Levitus et al.* [1994]. Data for heat flux (Q_{obs}), the coupling coefficient ($[\partial Q/\partial T]_{\mathrm{obs}}$), SST, and wind stress have been taken from the analysis by *Barnier et al.* [1995] of European Centre for Medium-Range Weather Forecasts (ECMWF) data for the years 1986–1988. This data set also provides the friction velocity that is necessary for the *Gaspar et al.* [1990] mixed-layer model as a boundary condition for TKE. The coupling coefficient, whose typical value is ~30 W K^{-1} m^{-2}, is calculated by evaluating derivatives with respect to T at each location in the empirical and theoretical equations used for estimating air-sea exchange of heat flux [*Haney*, 1971]. The above formulation (1) is advantageous to a pure restoring to observed SSTs as it converges to the correct surface heat flux as the model approaches correct SSTs.

[11] Experiment daily climatology (DC) is the same as MC, except that intraseasonal anomalies are superimposed on the "climatological" forcing fields. The anomalies are determined using daily averaged heat fluxes, wind stresses, and weekly averaged SST distributed by the National Center for Atmospheric Research/National Centers for Environmental Prediction (NCAR/NCEP) reanalysis project [*Kalnay et al.*, 1996] (available at http://www.cdc.noaa.gov/cdc/data.nmc.reanalysis.html). Weekly averaged SST is used because basin-wide daily maps are not available due to insufficient data coverage, in particular due to cloud-cover gaps in the satellite data. Intraseasonal components of wind stresses, Q_{obs}, and $\mathrm{SST}_{\mathrm{obs}}$ for the year 1987 are extracted from the reanalysis by subtracting the NCAR/NCEP data smoothed with a 31-day running mean filter from the original data. Monthly means of the cube of the friction velocity, u_*^3, are calculated from the daily wind stress τ via $u_* = (\tau/\rho)^{1/2}$, where ρ denotes the density of

seawater. Anomalies of u_*^3 are determined in the same manner as for the other forcing fields. The coupling coefficient $(\partial Q/\partial T)_{obs}$ was kept the same as in Experiment MC. Because this coefficient represents a property of a water column and the atmosphere above, namely, the sensitivity of heat flux to water temperature change, and is typically associated with monthly timescales (for a ML depth of, say, 50 m), it is not very meaningful to vary this coefficient on a timescale much shorter than a month.

[12] Experiment DY (daily, years 1994–1995) is forced with actual NCAR/NCEP data for the years 1994–1995, which include the period of the mooring observations at 15.5°N, 61.5°E (October 1994 through October 1995) [*Weller et al.*, 1998; *Dickey et al.*, 1998]. From 16 October 1994 to 20 October 20 1995, surface forcing data from the mooring site are merged into the NCAR/NCEP data so that the forcing at the mooring site is exactly the same as the observed one and the contribution of the mooring data decreases exponentially with distance with an e-folding scale of 500 km [*McCreary et al.*, 2001]. Monthly averages of the above data are calculated and used to drive Experiment MY (monthly, years 1994–1995). (The reader might want to refer to Figure 5 for how the monthly and the daily forcings compare with each other.)

[13] For the first two experiments in Table 1, the coupled model is integrated for 3 years after a 30-year stand-alone spin-up of the physical part. The choice of 3 years for the integration period is made because it is much longer than typical timescales implied by the parameter values of the ecosystem model (days to weeks). For the upper ocean, a stationary cycle is well established for the ecosystem model after 3 years of integration. For further discussion on the choice of the integration period, the reader is referred to *Kawamiya and Oschlies* [2003].

[14] The states of MC and DC at the end of the first year of integration are used as the initial conditions for MY and DY, respectively, which are then integrated for another 2 years with corresponding data for 1994–1995. The four main experiments are classified into two groups, that is, one composed of MC and DC and one of MY and DY, in each of which the only difference between the two experiments is the inclusion of intraseasonal variations. Unless specified otherwise, results are shown for the third year of integration.

3. Results

[15] A comparison of the results of the coupled ecosystem-circulation model with observations and other modeling studies and a discussion of critical processes for the pelagic ecosystem has been conducted in previous work [*Kawamiya*, 2001; *Kawamiya and Oschlies*, 2003]. In the following, we therefore concentrated on differences among the different model simulations of Table 1.

3.1. Experiments Based on Climatology

[16] Figures 1a–1d display the annual cycles of chlorophyll and vertical diffusion coefficient from Experiments MC and DC at the mooring site. The vertical diffusion coefficients in DC exhibit pronounced responses to the intraseasonal variations in forcing, yielding blooms in late February and August that are not seen in MC. The sharper deepening of the ML in the beginning of July in DC makes the corresponding bloom more intense.

[17] These differences, however, have little impact on biological fluxes on an annual basis. Simulated annual primary production at this site shows a difference of <5% (116 g C/m^2 for MC, 122 g C/m^2 for DC; see Figure 3a). Also, the prominent feature of the deep chlorophyll maximum (DCM) formation at depths of 50–70 m during the intermonsoon seasons (March–May and October–November) remains almost intact. The effect of intraseasonal variation is restricted to its own timescale (less than a few weeks) and does not map onto longer timescales. It appears that this is also the case for other regions of the Arabian Sea, and basin-scale distributions of annual primary production from the two experiments resemble each other (Figures 1e and 1f; see also Figure 3b).

3.2. Experiments Based on Data From 1994 to 1995

[18] Figures 2a–2d depict the annual cycles of chlorophyll and the vertical diffusion coefficient from Experiments MY and DY. Here the model is driven by NCAR/NCEP data for 1994–1995 on monthly and daily mean basis, respectively. The results are shown for the year 1995, namely, the third year of coupled integration. Many of the statements made for Figure 1 are equally valid for Figure 2: Responses of vertical mixing to intraseasonal variations are evident, without which some of the blooms in Figure 2b would not take place; annual primary production is, however, not significantly different (~223 g C/m^2 for both; see Figure 3a), and the DCM forms during the spring intermonsoon season. The resemblance between experiments with and without intraseasonal variations is retained also for the basin-scale distribution of annual primary production.

[19] Disagreements between Experiments DY and MY are, however, more noticeable than in the case with "climatological" forcing (DC and MC). In particular, the DCM does not form in MY in the fall intermonsoon season due to the deeper mixing in this experiment; the bloom at the end of the winter season lasts longer and that at the beginning of summer starts earlier in DY, with both the blooms split into a few short-lived subblooms. These differences suggest that taking into account intermittent surface forcing might be important for the interpretation of scarcely sampled data with a numerical model. However, high-frequency forcing in our experiments does not produce significant differences in annual production.

4. Discussion

4.1. Primary Production at the Mooring Site

[20] An intriguing finding is that at the mooring site, annual primary production in the experiments based on the forcing data from 1994–1995 (MY and DY) is almost doubled compared with those based on the *Barnier et al.* [1995] "climatology" run (MC and DC) as seen in Figure 3a. This difference, however, is a local phenomenon, and primary production integrated over the Arabian Sea is almost the same between the experiments forced using the "climatology" and the 1994–1995 data (Figure 3b). Comparison between Figures 1e and 1f and 2e and 2f indeed reveals that the mooring site (15.5°N, 61.5°E) is located where the difference is exceptionally large.

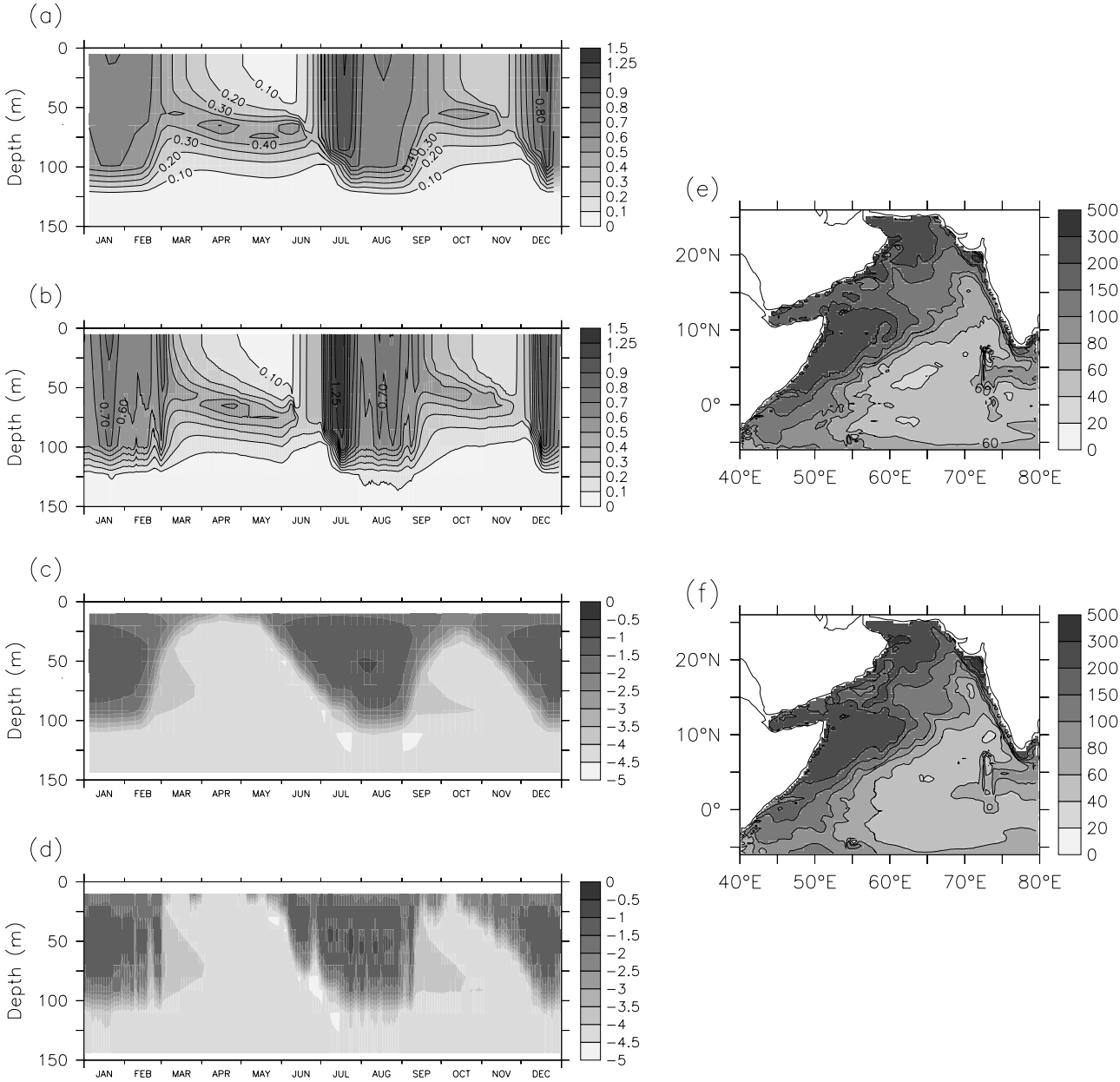

Figure 1. Seasonal variation of the modeled chlorophyll at 15.5°N, 61.5°E (corresponding to the WHOI mooring site) in Experiments (a) MC and (b) DC. Units are mg/m^3. Scale is the same as in Figure 2. Seasonal variation of the modeled vertical diffusion coefficient at the same site in Experiments (c) MC and (d) DC. Values are expressed with the common logarithm of those in m^2/s. Modeled annual primary production of the Arabian Sea in (e) MC and (f) DC. Units are g C/m^2. See Table 1 for description of the experiments.

[21] Two factors may be responsible for this difference. First, the annual mean Ekman upwelling velocity is negative in the case with "climatological" forcing at the mooring site (∼−5 cm/d), while it is positive with the 1994–1995 data (∼1 cm/d for 1994, ∼5 cm/d for 1995). The nitracline is lifted up with the 1994–1995 wind and more nitrate is entrained into the ML, although maximum mixed-layer depths (MLDs) during monsoon seasons remain unchanged for the different forcing data (Figures 1c and 1d and 2c and 2d). Second, the along-shore wind stress during SWM is stronger in the 1994–1995 data, whereby elevated nitrate concentrations occur along the coast of Oman during SWM. Typical nitrate concentrations are ∼10 mmol/m^3 for climatological forcing and ∼20 mmol/m^3 for the forcing using 1994–1995 data. Lateral transport of the upwelled nitrate mainly by mesoscale currents [*Kawamiya*, 2001] to the mooring site results in the enhancement of primary production for the 1994–1995 data.

[22] In contrast to the changes brought about by different background (monthly mean) averaged winds, changes due to including intraseasonal variations are quite small. While intraseasonal variations are essential for reproducing many

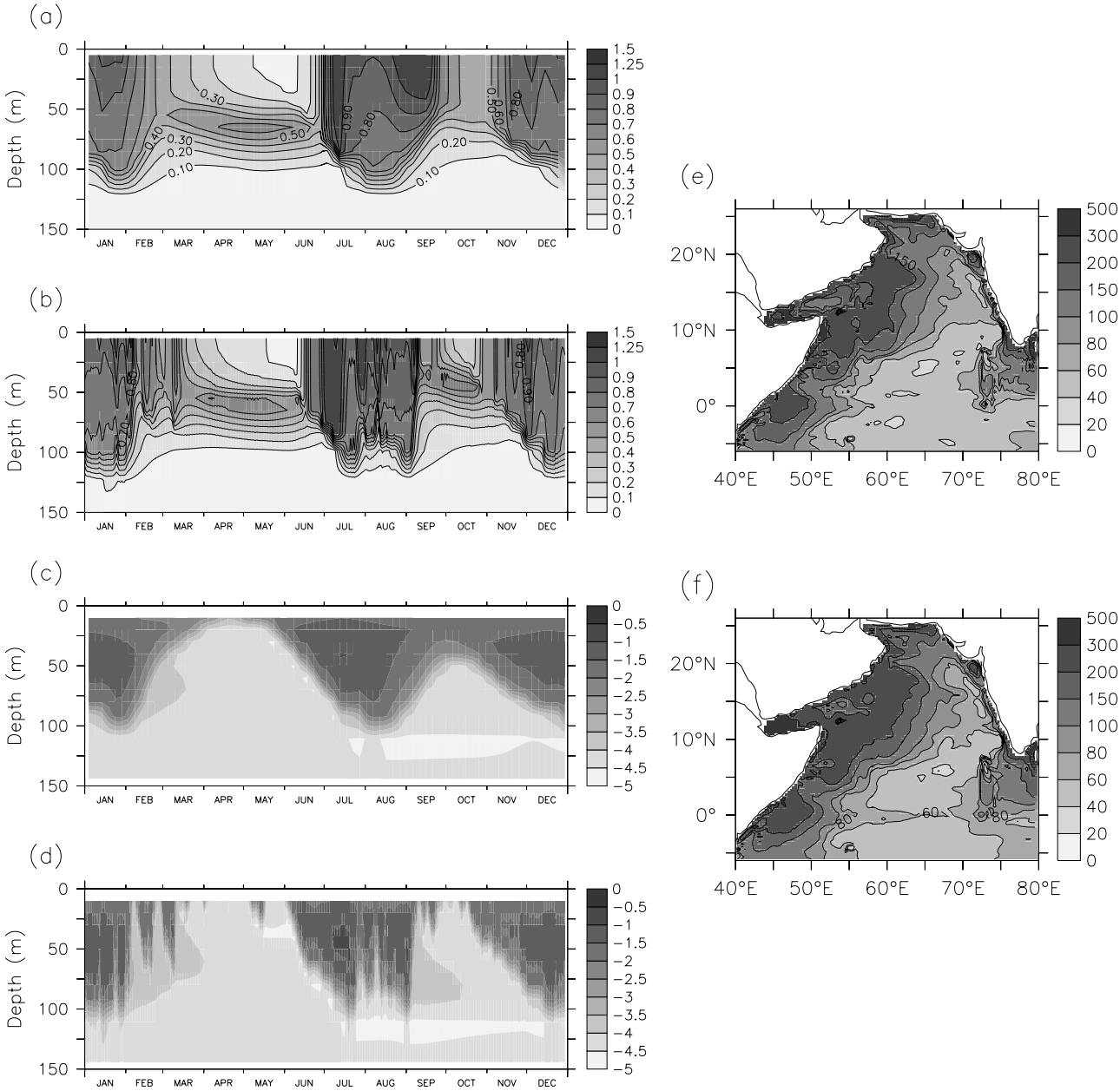

Figure 2. Same as in Figure 1. Seasonal variation of the modeled chlorophyll in Experiments (a) MY and (b) DY, seasonal variation of the modeled vertical diffusion coefficient in (c) MY and (b) DY, and modeled annual primary production in (e) MY and (f) DY.

of the short-term phytoplankton blooms seen in Figures 1b and 2b, their effect is restricted to their own timescale and does not propagate to longer timescales. A. Oschlies (personal communication, 2002) also carried out an experiment on the effect of intraseasonal variations using a similar ecosystem-circulation model for the Atlantic and obtained similar results.

[23] A possible explanation for this insensitivity is that primary production depends mainly on total upwelling, including both the open ocean Ekman pumping and the coastal upwelling, which in turn depends only on the background winds. Another factor is that on an intraseasonal timescale, subsurface nutrient replenishment following a mixed-layer retreatment is not rapid enough in our model to accumulate sufficient nitrate for a phytoplankton bloom to occur with the subsequent deepening of the mixed layer.

4.2. Comparison With Observations

[24] Measurements with fine time resolutions of the order of 10 min were conducted at the Woods Hole Oceanographic Institution (WHOI) mooring site [*Weller et al.*, 1998; *Dickey et al.*, 1998] from October 1994 to October 1995. Model results from Experiments MY and DY (those with the 1994–1995 data) are compared with the data to check the model performance in Figure 4 for the MLD and primary production. The MLD is defined as the depth at which the temperature difference from the sea surface first exceeds the critical value of 0.1°C. It is seen that DY reproduces the

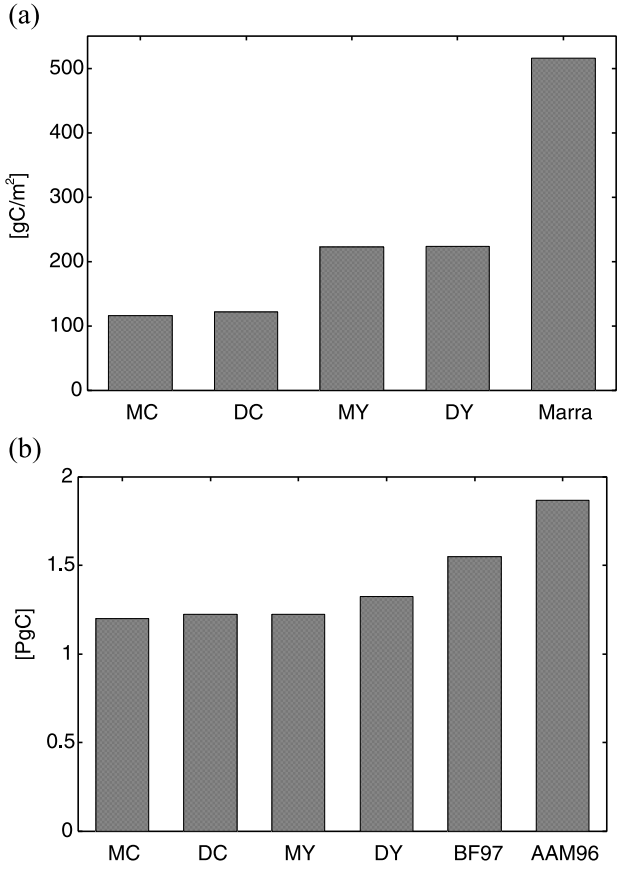

Figure 3. Annual primary production (a) at the WHOI mooring site (15.5°N, 61.5°E) from the model experiments and the observational estimate based on fluorescence and surface irradiance by Marra et al. [1998] (denoted as Marra), and (b) integrated over the entire Arabian Sea (5°S–25°N, 40°E–80°E) from the model experiments and satellite-based estimates by *Behrenfeld and Falkowski* [1997] (denoted BF97) and *Antoine et al.* [1996] (AAM96). See Table 1 for description of the experiments.

observed MLD rather well, including short-term variations such as those in February and March. Discrepancies are found during October–November and July–August. The ML deepening in the former and shallowing in the latter are, however, known to be caused by mesoscale currents [*Dickey et al.*, 1998], and it cannot be expected that the model bears the same behavior of ML in these periods because of the chaotic nature of mesoscale currents. Experiment MY yields an MLD variation that follows the general trend in that of DY on a seasonal timescale except for September–October 1995, during which the MLDs of MY are consistently deeper by ~20 m. Although a computation of the Monin-Obukhov length as defined by *McCreary et al.* [2001] suggests that the MLD should be ~20 m in October also in MY, TKE calculated by the *Gaspar et al.* [1990] mixed-layer model does not immediately vanish at depths of ~50 m even after SWM ceases, and thus the vertical mixing coefficient there stays moderately high ($\sim 5 \times 10^{-3}$ m^2/s; Figure 2c). At the end of the SWM season, the TKE loss through the energy conversion term is smaller than it is at the end of the northeastern monsoon season (NEM) because of the different processes involved: The main factor for the ML shoaling at the end of the SWM season is the weakening of the wind stirring while the ML shoaling at the end of the NEM season is caused by the surface warming, which is associated with stratification and a higher transfer of TKE into potential energy.

[25] Simulated primary production does not compare so favorably with the observational estimate by *Marra et al.* [1998] based on fluorescence and surface irradiance. The model often underestimates primary production by a factor of 2 or more. The discrepancy is largest during the periods of enhanced primary production in the data, that is, December, February–March, and September. The observed peak during December is associated with an arrival of a mesoscale current [*Dickey et al.*, 1998], which can play an important role in horizontal transport of nitrate [*Kawamiya*, 2001]. The passage of a mesoscale current is a chaotic phenomenon, as mentioned earlier, and its accurate prediction with a numerical model is difficult to achieve without data assimilation and cannot be expected here.

[26] The broad peak in observed primary production during February–March seems to be caused by improving light conditions due to the ML retreat in this period. For an enhancement of primary production to occur with a ML retreat, an adequate amount of nitrate needs to be accumulated beforehand. The model may fail to represent the nitrate accumulation at this site correctly. For example, *Kawamiya* [2001] indeed found that the simulated activity of mesoscale currents is lower than estimated based on satellite data of sea surface height, which may result in an underestimate of horizontal transport of nitrate initially upwelled along the coast of Oman to the offshore region.

[27] The observed primary production peak during September may also be caused by the retreat of the ML. The magnitude of the retreat is, however, relatively small (from ~60 m to ~20 m) for such a drastic enhancement of primary production. In this respect, it is noteworthy that the observed water-column heat budget at this site carries an oscillatory feature and cannot be closed closely during this period [see *Fischer et al.*, 2002, Figure 4]. There may therefore be a significant contribution from horizontal heat transport by mesoscale currents during this period, which may also be relevant to the peak in primary production.

[28] The frequent underestimate of primary production by the model including the lack of the three conspicuous peaks in the data leads to an annual primary production less than a half of the observational estimate (Figure 3a). Experiment MY again yields a variation of primary production that follows the general trend in that of DY on a seasonal timescale except for September–October, when the ML is constantly deeper in MY. It should be pointed out that reproducing primary production at this site may be extremely difficult due to strong horizontal gradient around the site, as seen in the primary production field of satellite-based estimates [cf. *Kawamiya and Oschlies*, 2003, Figure 10], and possible interannual variability indicated by the factor-of-2 difference between, for example, DC and DY (Figure 3a).

[29] While the mooring site might be a place where disagreement between the model and observations is exceptionally large, basin-averaged annual primary production in the model experiments is closer to, though still smaller than, the satellite-based estimates by *Behrenfeld and Falkowski*

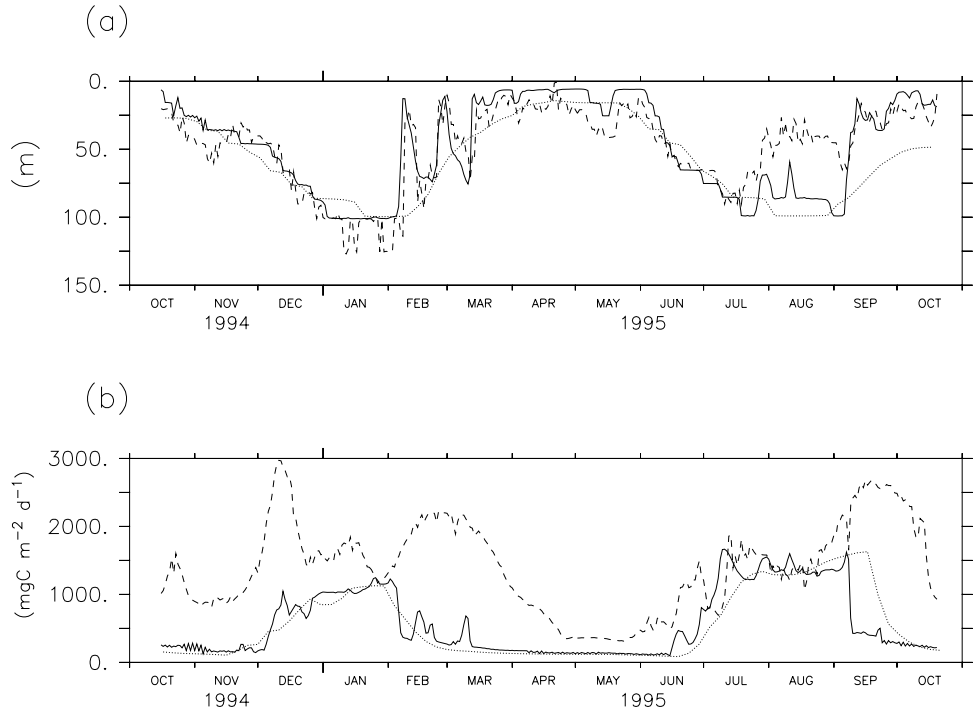

Figure 4. (a) Mixed-layer depth (MLD) at the WHOI mooring site (15.5°N, 61.5°E) for Experiments DY (solid line), MY (dotted line), and the data (dashed line). The MLD is defined as the depth at which the temperature difference from the sea surface first exceeds the critical value of 0.1°C. For the data, daily maxima are taken as the MLD values of the corresponding days. (b) Same as in Figure 4a but for vertically integrated primary production. The data are from the estimate based on fluorescence and surface irradiance by *Marra et al.* [1998]. See Table 1 for description of the experiments. Data are available from the Web site of the Arabian Sea Test Bed maintained by K. E. Kohler, R. R. Hood, and J. P. McCreary (http://www.nova.edu/cwis/oceanography/arabsea/testbed/testbed.html).

[1997] and *Antoine et al.* [1996] (Figure 3b). A similar underestimate was found in an application of essentially the same marine ecosystem model to the North Atlantic, which, however, closely fit observational estimates of nutrient supply or new production [*Oschlies*, 2002]. Accordingly, the underestimation of total primary production may be caused by underestimated regenerate production.

[30] Given the model's underestimate of primary production at the mooring site, one might well expect that the influence of intraseasonal variations is also underestimated. However, as the underestimated total primary production is likely a result of underestimated regenerated production (i.e., a too high *f*-ratio), the effect of short-term fluctuations of the ML to pump up nutrient should result in relative changes in primary production being overestimated rather than underestimated. In fact, the amplitude of the simulated response of primary production to short-term fluctuations of the ML in, for example, February and March, is even in absolute units slightly larger than that in the data (Figure 4). There is thus little indication that the too low background values of simulated primary production may reflect an underestimation of the effect of intraseasonal variations at the mooring site.

4.3. Causes for the Variations of the MLD

[31] Since intraseasonal variations have proved to be effective enough to produce short-term blooms that do not appear when monthly-mean forcing is used, it is also an interesting question, Which of wind stress and heat flux is responsible for generating fluctuations of the MLD associated with these blooms? To examine this, two sensitivity experiments are performed as shown in Table 1. Both are similar to Experiment DY, which is forced with daily mean data, but DY-S1 is forced with monthly mean heat flux and DY-S2 is forced with monthly mean wind stress and friction velocity. The MLDs at the mooring site from the three experiments DY, DY-S1, and DY-S2 are compared in Figure 5a for the same period as in Figure 4, with the corresponding monthly and daily data for wind stress and total heat flux depicted in Figures 5b and 5c.

[32] From October 1994 to the middle of May 1995, the MLDs from DY-S2 (green line) are more similar to those from DY (black) in that they duplicate the two major fluctuations during February to early March, meaning that during this period variations in heat flux are more relevant than those in wind. The opposite is true between the middle of May and September 1995, i.e., the MLDs of Experiment DY fluctuate more in phase to those of DY-S1 (red). In October 1995, Experiment DY again yields MLDs closer to those of DY-S2. This result is rather intuitive in that variations in wind are most important when the wind fluctuates with largest amplitudes. The impact of short-term fluctuations in the heat flux on the MLD, on the other hand, is strongest when the wind fluctuations are relatively weak and the TKE production rate [e.g., *McCreary et al.*, 2001]

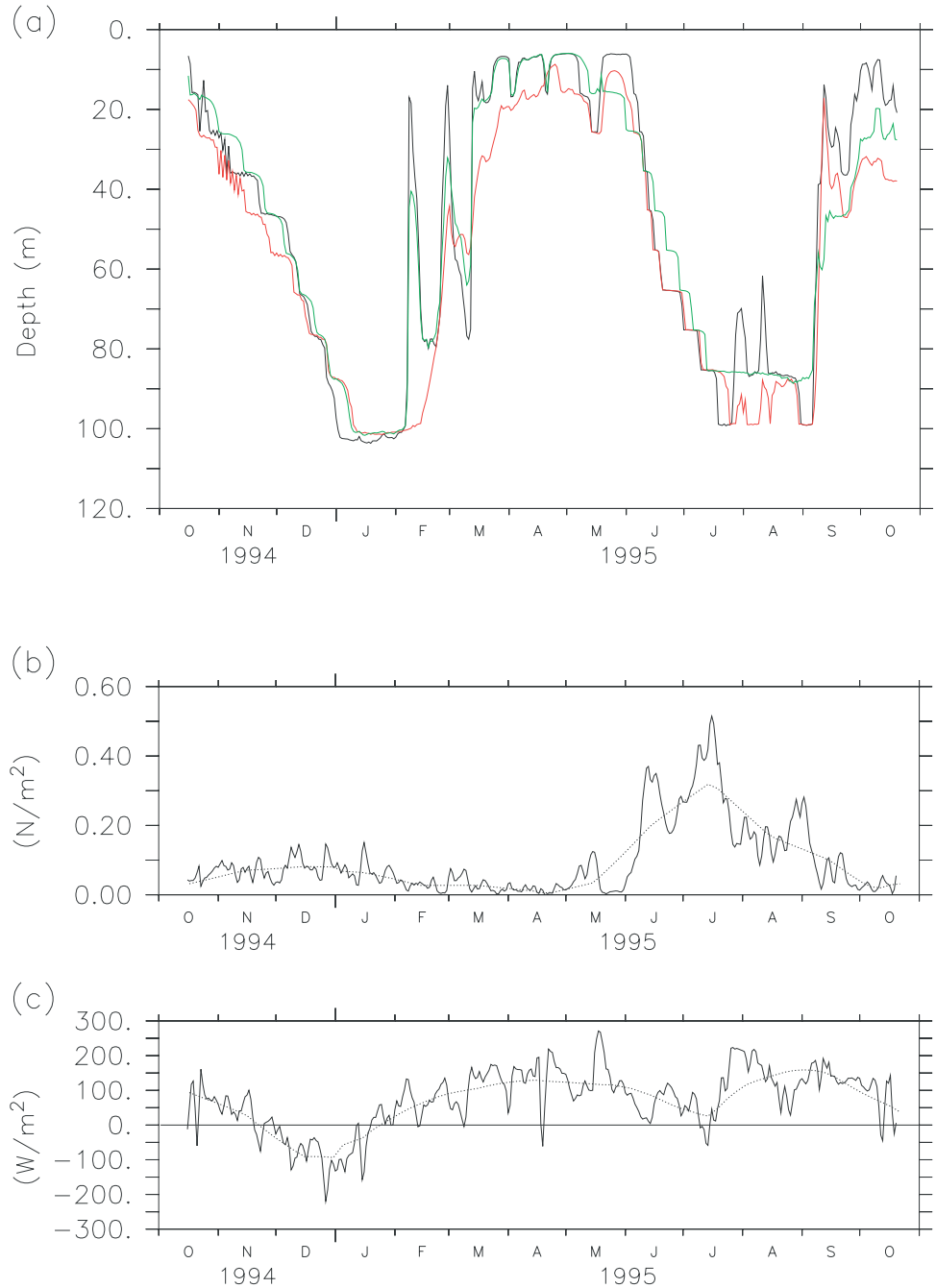

Figure 5. (a) Mixed-layer depth at the WHOI mooring site (15.5°N, 61.5°E) for Experiments DY (black line, the same as the solid line in Figure 4a), DY-S1 (red), and DY-S2 (green). (b) Wind stress and (c) total heat flux calculated by equation (1) at the same site. In Figures 5b and 5c the solid lines represent daily data and dotted lines represent monthly data. See Table 1 for description of the experiments.

changes its sign because of fluctuation in the heat flux as in February and March 1995. When attempting to interpret MLD variations in terms of surface fluxes, and to thereby associate chlorophyll variations with atmospheric conditions at this site, it would therefore be more illuminating to look at heat flux during October to the middle of May and wind stress during the rest of the year. As to which of wind speed and direction is more important for creating the MLD variations, we conclude that at the mooring site the former is essential because calculating Monin-Obukhov length as defined by *McCreary et al.* [2001] was found to reproduce most of the short-term variations of the MLD.

5. Conclusions

[33] The impact of intraseasonal variations of surface buoyancy flux and wind stress on the pelagic ecosystem has been investigated using an ecosystem-circulation model of the Arabian Sea. A series of experiments has been carried out using surface forcing data with and without intra-

seasonal variations. When forced with intraseasonal variations, the experiments show ML responses to fluctuations in surface forcing, which may be driven mainly by heat flux during October to the middle of May and by wind during the rest of the year, thereby producing short-term phytoplankton blooms not seen in the experiments forced without them. These blooms can extend the overall duration of periods with high chlorophyll concentrations, as was also found by *McCreary et al.* [2001]. This suggests that the intraseasonal variation is important if time series data are to be interpreted using a numerical model. The comparison among the experiments with and without intraseasonal variations reveals, however, that those short-term blooms do not generate a significant enhancement of annual primary production at the mooring site or over the entire Arabian Sea. The overall pattern of seasonal variation in primary production at the mooring site also remains similar among the experiments.

[34] We note that results might well be different for other regions of the ocean and that more complex ecosystem models, for example, with competing species of the same functional group, may be more sensitive to high-frequency forcing. In this particular series of experiments, however, the impact of intraseasonal variations is felt mainly on the timescale of the variations. For longer timescales, changes associated with differences in surface forcing on a seasonal timescale are greater. The model may be forced with monthly data without a serious loss of its ability whenever the focus is on the biogeochemical nutrient cycling on seasonal or longer timescales.

[35] **Acknowledgments.** This work is a contribution to the German JGOFS Program. We thank J. P. McCreary and the anonymous reviewers for their constructive comments that helped to improve the paper. M.K. has benefited from financial support from Frontier Research System for Global Change, JAMSTEC, to complete this work.

References

Antoine, D., J.-M. André, and A. Morel (1996), Oceanic primary production: 2. Estimation at global scale from satellite (coastal zone color scanner) chlorophyll, *Global Biogeochem. Cycles*, *10*, 57–69.

Barnier, B., L. Siefridt, and P. Marchesiello (1995), Surface thermal boundary condition for a global ocean circulation model from a three-year climatology of ECMWF analysis, *J. Mar. Syst.*, *6*, 363–380.

Behrenfeld, M. J., and P. G. Falkowski (1997), Photosynthetic rates derived from satellite-based chlorophyll concentration, *Limnol. Oceanogr.*, *42*, 1–20.

Blanke, B., and P. Delecluse (1993), Variability of the tropical Atlantic Ocean simulated by a general circulation model with two different mixed-layer physics, *J. Phys. Oceanogr.*, *23*, 1363–1388.

Dickey, T., J. Marra, D. E. Sigurdson, R. A. Weller, C. S. Kinkade, S. E. Zedler, J. D. Wiggert, and C. Langdon (1998), Seasonal variability of bio-optical and physical properties in the Arabian Sea: October 1994–October 1995, *Deep Sea Res., Part II*, *45*, 2001–2025.

Fischer, A. S., R. A. Weller, D. L. Rudnick, C. C. Eriksen, C. M. Lee, K. H. Brink, C. A. Fox, and R. R. Leben (2002), Mesoscale eddies, coastal upwelling, and the upper-ocean heat budget in the Arabian Sea, *Deep Sea Res., Part II*, *49*, 2231–2264.

Gaspar, P., Y. Grégoris, and J.-M. Lefevre (1990), A simple eddy kinetic energy model for simulations of the oceanic vertical mixing: Tests at Station Papa and Long-Term Upper Ocean Study site, *J. Geophys. Res.*, *95*, 16,179–16,193.

Haney, R. L. (1971), Surface thermal boundary condition for ocean circulation models, *J. Phys. Oceanogr.*, *1*, 241–248.

Kalnay, E., et al. (1996), The NCEP/NCAR 40-year reanalysis project, *Bull. Am. Meteorol. Soc.*, *77*, 437–471.

Kawamiya, M. (2001), Mechanism of offshore nutrient supply in the western Arabian Sea, *J. Mar. Res.*, *59*, 675–696.

Kawamiya, M., and A. Oschlies (2003), An eddy-permitting, coupled ecosystem-circulation model of the Arabian Sea: Comparison with observations, *J. Mar. Syst.*, *38*, 221–257.

Large, W. G., and G. B. Crawford (1995), Observations and simulations of upper-ocean response to wind events during the ocean storms experiment, *J. Phys. Oceanogr.*, *25*, 2831–2852.

Levitus, S., R. Burgett, and T. P. Boyer (1994), *World Ocean Atlas 1994*, vol. 3, *Salinity*, NOAA Atlas NESDIS 3, U.S. Govt. Print. Off., Washington, D. C.

Marra, J., T. D. Dickey, C. Ho, C. S. Kinkade, D. E. Sigurdson, R. A. Weller, and R. T. Barber (1998), Variability in primary production as observed from moored sensors in the central Arabian Sea in 1995, *Deep Sea Res., Part II*, *45*, 2253–2267.

McCreary, J. P., K. E. Kohler, R. R. Hood, and D. B. Olson (1996), A four-compartment ecosystem model of biological activity in the Arabian Sea, *Prog. Oceanogr.*, *37*, 193–240.

McCreary, J. P., K. E. Kohler, R. R. Hood, S. Smith, J. Kindle, A. S. Fischer, and R. A. Waller (2001), Influences of diurnal and intraseasonal forcing on mixed-layer and biological variability in the central Arabian Sea, *J. Geophys. Res.*, *106*, 7139–7155.

Oschlies, A. (2002), Nutrient supply to the surface waters of the North Atlantic: A model study, *J. Geophys. Res.*, *107*(C5), 3046, doi:10.1029/2000JC000275.

Oschlies, A., and V. Garçon (1999), An eddy-permitting coupled physical-biological model of the North Atlantic: 1. Sensitivity to advection numerics and mixed layer physics, *Global Biogeochem. Cycles*, *13*, 135–160.

Pacanowski, R. C. (1995), MOM 2 documentation: User's guide and reference manual, *Tech. Rep. 3*, Geophys. Fluid Dyn. Lab., Princeton, N. J.

Pacanowski, R. C., and S. G. H. Philander (1981), Parameterization of vertical mixing in numerical models of tropical oceans, *J. Phys. Oceanogr.*, *11*, 1443–1451.

Ridderinkhof, H. (1992), On the effects of variability in meteorological forcing on the vertical structure of a stratified water column, *Cont. Shelf Res.*, *12*, 25–36.

Rix, N. H. (1998), Investigating Indian Ocean variability in a basin scale GCM: Model assessment and model-data intercomparison, Ph.D. thesis, 155 pp., Universität Kiel, Kiel, Germany.

Weller, R. A., M. F. Baumgartner, S. A. Josey, A. S. Fischer, and J. C. Kindle (1998), Atmospheric forcing in the Arabian Sea during 1994–1995: Observations and comparisons with climatology and models, *Deep Sea Res., Part II*, *45*, 1961–1999.

M. Kawamiya, Frontier Research System for Global Change, 3173-25, Showamachi, Kanazawa-ku, Yokohama, 236-0001, Japan. (kawamiya@jamstec.go.jp)

A. Oschlies, Institut für Meereskunde an der Universität Kiel, Düsternbrooker Weg 20, 24105, Kiel, Germany.